Design and simulation of high-speed nanophotonic electro-optic modulators

S.N. Kaunga-Nyirenda[1], H.K. Dias[1], J.J. Lim[1], S. Bull[1], S. Malaguti[2], G. Bellanca[2] and E.C. Larkins[1]
[1]The University of Nottingham, University Park, Nottingham, NG7 2RD, U.K.
[2]University of Ferrara, Via Saragat, 1, Ferrara, 44122, Italy

***Abstract* – In this work, an ultracompact electro-optic modulator based on refractive index modulation by plasma dispersion effect in PhC all-optical gate (AOG) is proposed. The index modulation is achieved by applying a time-varying bias voltage across the electrical contacts of the AOG. The proposed modulator has potential for high-speed operation, with bandwidths in excess of 30GHz achievable.**

I. Introduction

The growth of ultra-high bandwidth applications has created a strong demand for photonic integrated circuits (PICs) with increased functionality, reduced footprint and power consumption [1-2]. Photonic crystal (PhC) technology is a promising candidate for such applications, due to its ultra-low power consumption and extreme compactness. Compact receivers and switching components are key devices in achieving optoelectronic integration. PhC All-optical gates (AOGs) and photodetectors are central building blocks for these components [2].

Nanophotonic electro-optic (EO) modulators have been demonstrated in compound semiconductors [3-6]. Mach-Zehnder EO modulators have been realised with ~80 μm PhC slow-light waveguides using both lateral carrier injection [3] and the thermo-optic effect [4]. Their switching contrast and wide optical bandwidth are attractive, but they have a large footprint (~100x100μm^2). High-speed (~3ps) optical switching has been demonstrated with a 10x10μm^2 directional coupler, but only with optical excitation [4]. EO modulators have also been realised with a variety of 1D and 2D PhC cavities with lateral p-i-n diodes for carrier injection [5,6], but the carrier transit time across the intrinsic region (typically 1-5μm) greatly limits their turn-on time, and the width and resistivity of the carrier injection region results in excess power dissipation. To avoid reliance on the plasma effect, polymer-filled slotted waveguides have been used to enhance Pockels effect for EO switching in silicon nanocavity modulators [7], but the switching performance (power and speed) remained unclear. We propose an electro-optic modulator based on a nanophotonic resonator with a lateral p-i-n diode to modulate the carrier plasma in the resonator using a CW pump beam to selectively generate carriers in the cavity via two photon absorption (TPA).

II. Device Operation

In the proposed EO modulator, the optical switching is only affected by the plasma density in the cavity, so the applied electric field only needs to move the carriers a comparatively short distance and the power dissipated by carrier generation is limited by the small cavity volume. As this device relies on TPA ($2*E_{ph} > 1.6$eV), it can also be used Si-based modulators. The advantages of this design over other integrated modulators include low power dissipation, higher reliability, low complexity and chirp-free operation.

Most applications in resonant cavity AOGs are achieved by changing of the cavities' resonant condition through refractive index changes. One of the main processes shown to be responsible for this refractive index change is the plasma dispersion effect, which is due to free carriers generated by TPA. The refractive index changes responsible for the resonant condition shift are usually modulated by switching on and off the pump optical power responsible for carrier generation through TPA. In the proposed device, the index change is achieved by applying a time-varying bias voltage across the electrical contacts. The time-varying bias results in modulation of the electric field across the cavity which changes the rate at which free carriers are swept away from the point of generation. The modulation of the carrier distributions leads to the modulation of the refractive index and hence the resonant condition of the cavity.

III. Description of Simulation Tool

Numerical modelling continues to play an important role in the design and development of novel device structures and technologies. Advanced simulation tools are required for the accurate, physics-based simulation of active nanophotonic devices. This is because their functionality is achieved by the perturbation of the dielectric response function (refractive index and/or gain (loss)) of the material. The dielectric response function is strongly dependent on the electron and hole densities. At the same time, the electron and hole distributions are strongly influenced by the optical fields through stimulated recombination, two-photon absorption (TPA) and free-carrier absorption (FCA) processes. A self-consistent dynamic simulation tool is required to accurately describe the coupled electronic, thermal and electromagnetic properties of active nanophotonics devices.

A dynamic 2D bipolar electrical/thermal solver [8] is bidirectionally coupled to an optical model. A complete description of problem would require a 3D FDTD-based optical model. However, a computationally efficient model based on coupled-mode theory (CMT), which has been calibrated by FDTD, is sufficient to investigate most important features. In the coupled electrical/CMT model (Fig. 1), the spatial distributions of the complex material polarisation are calculated from carrier and temperature distributions by the electrical/thermal model. The carrier-induced complex index change is appropriately averaged over the cavity volume and passed to the CMT model to calculate the instantaneous cavity resonance shift. Furthermore, the carrier distributions are averaged over the cavity mode volume in order to calculate the rate of energy dissipation due to FCA. The same procedure is followed in estimating the rate of energy dissipation in the cavity due to TPA. The CMT model in turn calculates the instantaneous energy in the cavity. This is passed to the electrical model, and scaled with respect to the cavity mode (obtained from FDTD calculations), in order to calculate the

978-1-4799-3682-3/14/$31.00 ©2014 IEEE

spatial distribution of the carrier generation rate.

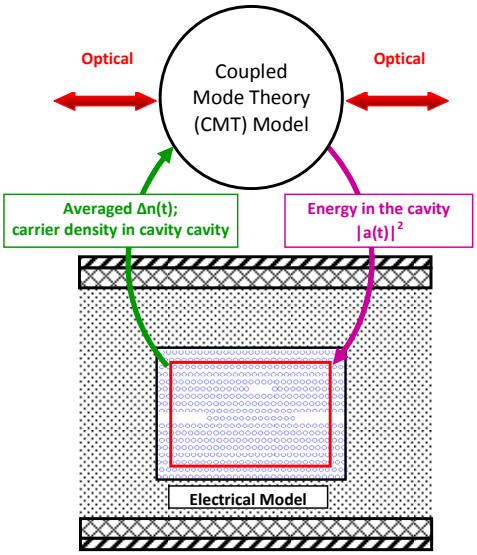

Fig. 1: *Block diagram of the coupling of the electrical-thermal model and the CMT model.*

The coupled CMT/electrical model has the advantage of being computationally more efficient than an FDTD solver so that longer simulations can be performed, while still faithfully representing its electrical response (including the use of electrical input signals/biases).

IV. Simulated Performance

The device used is an InP-based L3 cavity, with intrinsic and extrinsic Q-factors taken to be 300000 and 7000 respectively. The AOG was p-doped at 10^{16}cm^{-3}. Fig. 2 shows the time variation of the average electron density in the cavity as a function of pump powers (a), and applied voltage step (b).

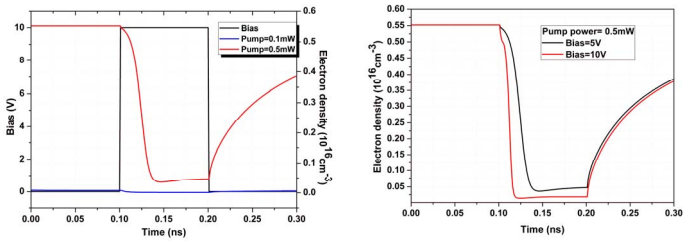

(a) (b)

Fig. 2: Time variation of the (a) electron density at 2 pump powers for 10V step, (b) electron density for 2 voltage steps for a pump power of 0.5W.

In the absence of an externally applied electric field, the carrier density remains at steady-state, so that the generation rate due to TPA balances the diffusion of carriers away from the cavity and carrier loss due to recombination. At the onset of the external electric field, the carriers are swept away from the cavity, so that the average carrier density drops. The rate at which the carrier distribution drops, as well as the depth it drops, are a function of both the pump power (which controls the rate of generation) and the strength of the applied electric field (which controls the rate at which the carriers are swept by the field away from the point of generation). To further appreciate the processes shown in Fig. 2, Fig. 3 shows snapshots of the electron current densities at two different time points during the voltage step.

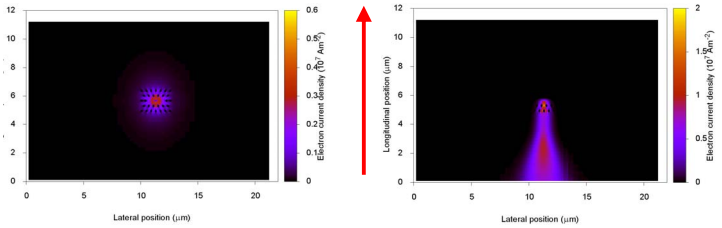

(a) (b)

Fig. 3: Electron current density maps at (a) 50ps; (b) 120ps. The voltage is applied at the bottom of the AOG. Red arrow indicates direction of applied electric field.

At the peak of the voltage pulse (b), a large current (holes flowing in the direction of the field, electrons flowing towards the positive electrode) can be observed showing that the field is sweeping the carriers away from the cavity. Fig. 4 shows the change in refractive index and the modulated output power as a function of time for a 10Gb/s bias voltage NRZ signal. The potential bandwidth (estimated from the rise/fall time) of the proposed modulator is in excess of 30GHz.

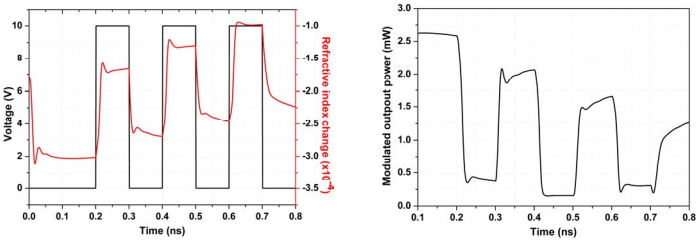

(a) (b)

Fig. 4: Refractive index change (a) and modulated output power (b) as a function of time for a 10Gb/s bias voltage signal.

V. Conclusions

We have demonstrated an ultracompact high-speed modulator using a coupled electrical/optical simulation tool. The high speed operation is achievable since the device operation is based on the rate of removing carriers from the point of generation faster than they are generated. Several performance metrics (e.g modulation depth, speed) will be further investigated. The simulation tool described will also be used to investigate other applications e.g. optical memories.

Acknowledgement

The authors gratefully acknowledge the EU Information Communication Technologies Framework 7 RTD Project COPERNICUS (IST- 249012).

References

[1] R. Nagarajan, et al, "Large-scale photonic integrated circuits," *IEEE J. Sel. Topics Quant. Electron.*, vol. **11**, (1), pp.50-65, 2005.

[2] M. Notomi et al: "Low-power nanophotonic devices based on photonic crystals towards dense photonic network on chip," *IET Circuits Devices Syst*, vol. **5** (2), pp. 84-93, 2011.

[3] Y. Jiang, et al, "80-micron interaction length silicon photonic crystal waveguide modulator," *Appl. Phys. Lett.* vol. **87**, 221105, 2005.

[4] L. O'Faolain, *et al*, "Compact optical switches and modulators based on dispersion engineered photonic crystals," *IEEE Phot. J.*, vol. **2**, pp. 404-414, 2010.

[5] B. Schmidt, et al, "Compact electro-optic modulator on silicon-on-insulator substrates using cavities with ultra-small modal volumes," *Opt. Exp.*, vol. **15**, pp. 3140-3148, 2007.

[6] T. Tanabe, et al, "Low power and fast electro-optic silicon modulator with lateral p-i-n embedded photonic crystal nanocavity," *Opt. Exp.*, vol. **17** (25), pp. 22505-22513.

[7] J.H. Wülbern, et al., "Electro-optic modulation in slotted resonant photonic crystal structures," *Appl. Phys. Lett.*, vol 94, 241107, 2009.

[8] J.J. Lim *et al*, "Static and dynamic performance optimisation of a 1.3μm GaInNAs ridge waveguide laser," *Opt Quant Electron*, vol. **40** (14-15), pp. 1181-1186, 2008.